ISSN 1936-8798/$36.00
PUBLISHED BY ELSEVIER INC.
DOI: 10.1016/j.jcin.2010.07.016

# A Comparison of the Conformability of Everolimus-Eluting Bioresorbable Vascular Scaffolds to Metal Platform Coronary Stents

Josep Gomez-Lara, MD,* Hector M. Garcia-Garcia, MD, PhD,*† Yoshinobu Onuma, MD,* Scot Garg, MB, ChB,* Evelyn Regar, MD, PhD,* Bernard De Bruyne, MD, PhD,‡ Stefan Windecker, MD,§ Dougal McClean, MD,‖ Leif Thuesen, MD,¶ Dariusz Dudek, MD,# Jacques Koolen, MD, PhD,** Robert Whitbourn, MD,†† Pieter C. Smits, MD, PhD,‡‡ Bernard Chevalier, MD,§§ Cécile Dorange, MSc,‖‖ Susan Veldhof, RN,‖‖ Marie-Angèle Morel, BSc,† Ton de Vries, MSc,† John A. Ormiston, MB, ChB, PhD,¶¶ Patrick W. Serruys, MD, PhD*

*Rotterdam and Eindhoven, the Netherlands; Aalst and Diegem, Belgium; Bern, Switzerland; Christchurch and Auckland, New Zealand; Skejby, Denmark; Krakow, Poland; Fitzroy, Australia; and Massy, France*

**Objectives** The aim of this study was to assess the differences in terms of curvature and angulation of the treated vessel after the deployment of either a metallic stent or a polymeric scaffold device.

**Background** Conformability of metallic platform stents (MPS) is the major determinant of geometric changes in coronary arteries caused by the stent deployment. It is not known how bioresorbable polymeric devices perform in this setting.

**Methods** This retrospective study compares 102 patients who received an MPS (Multi-link Vision or Xience V, Abbott Vascular, Santa Clara, California) in the SPIRIT FIRST and II trials with 89 patients treated with the Revision 1.1 everolimus-eluting bioresorbable vascular scaffold (BVS) (Abbott Vascular, Santa Clara, California) from cohort B of the ABSORB (A bioabsorbable everolimus-eluting coronary stent system) trial. All patients were treated with a single 3 × 18 mm device. Curvature and angulation were measured with dedicated software by angiography.

**Results** Both the MPS and BVS groups had significant changes in relative region curvature (MPS vs. BVS: 28.7% vs. 7.5%) and angulation (MPS vs. BVS: 25.4% vs. 13.4%) after deployment. The unadjusted comparisons between the 2 groups showed for BVS a nonsignificant trend for less change in region curvature after deployment (MPS vs. BVS: 0.085 $cm^{-1}$ vs. 0.056 $cm^{-1}$, $p = 0.06$) and a significantly lower modification of angulation (MPS vs. BVS 6.4° vs. 4.3°, $p = 0.03$). By multivariate regression analysis, the independent predictors of changes in curvature and angulation were the pre-treatment region curvature, the pre-treatment region angulation, and the used device.

**Conclusions** Bioresorbable vascular scaffolds have better conformability than conventional MPS. The clinical significance of the observed differences will require further investigation. (J Am Coll Cardiol Intv 2010;3:1190–8) © 2010 by the American College of Cardiology Foundation

From the *Thoraxcenter, Erasmus Medical Center, Rotterdam, the Netherlands; †Cardialysis, Rotterdam, the Netherlands; ‡Cardiovascular Center, Aalst, Belgium; §Swiss Cardiovascular Center, Bern, Switzerland; ‖Christchurch Hospital, Christchurch, New Zealand; ¶Skejby Sygehus, Aarhus University Hospital, Skejby, Denmark; #Jagiellonian University, Krakow, Poland; **Catharina Ziekenhuis, Eindhoven, the Netherlands; ††St. Vincent's Hospital, Fitzroy, Australia; ‡‡Maasstad Ziekenhuis, Rotterdam, the Netherlands; §§Institut cardio-vasculaire Paris-Sud, Massy, France; ‖‖Abbott Vascular, Diegem, Belgium; and the ¶¶Auckland City Hospital, Auckland, New Zealand. The ABSORB cohort B and the SPIRIT I and II trials have been supported by Abbott. The authors are also grateful to the Spanish Society of Cardiology for the grant awarded to the first author. Dr. Ormiston is on the advisory board and received honoraria from Boston Scientific and Abbott Vascular. Dr. Smits received a research grant and speakers fees from Abbott Vascular. Dr. Windecker received lecture and consultant fees from Abbott, Biosensors, Boston Scientific, Cordis, and Medtronic. Drs. Veldhof and Dorange are employees of Abbott Vascular. Dr. Dudek is an advisory board member and speaker of Abbott Vascular. All other authors have reported that they have no relationships to disclose.

Manuscript received February 24, 2010; revised manuscript received June 29, 2010, accepted July 10, 2010.

Coronary arteries have variable anatomies that are dynamically changing in morphology through the heart cycle. Acute changes in the geometry of coronary arteries after implantation of rigid metallic stents can be related to clinical outcomes (1). It has been suggested that this interaction can be explained by the alteration of the flow rheology within the vessel (2,3) and by the increased risk of stent fracture in angulated lesions (4). The most important device property that determines these changes in vessel geometry is the conformability of the stent (5). It is described as the flexibility of a stent in its expanded state with adaptation to the natural shape of the vessel, hence minimizing trauma to the vessel wall (6). Stent conformability is dependent on both the material and design of the stent and is therefore different between the commercial devices that are available (7,8).

See page 1199

A bioresorbable device capable of providing temporary scaffolding without changing the vessel geometry would be highly desirable in order to prevent complications related to the permanent presence of metal as stent thrombosis, and probably, those complications due to changes in vessel curvature such as restenosis or stent fracture. The everolimus-eluting bioresorbable vascular scaffold (BVS) (Abbott Vascular, Santa Clara, California) is a new generation of intracoronary devices that is currently under investigation in the ongoing ABSORB (A bioabsorbable everolimus-eluting coronary stent system) trial (9,10). Results so far demonstrate favorable clinical outcomes out to 3-year follow-up (11); however, the acute effects of its implantation on vessel geometry are yet to be investigated. Therefore, our aim is to compare the effects of the BVS on coronary vessel geometry compared with metallic platform stents (MPS).

## Methods

**Study design, population, and treatment device.** This nonrandomized, 2-arm, retrospective study has been performed with patients from the ABSORB Cohort B trial, and a subset of patients from the SPIRIT FIRST (12) and II (13) trials that received a Multi-link Vision metal platform stent (the bare-metal Vision or the drug-eluting Xience V stent; Abbott Vascular).

All patients in the ABSORB Cohort B trial were treated with a device 3.0 mm in diameter and 18 mm in length. Therefore, only those patients enrolled in the SPIRIT FIRST and II trials who received the same stent size were eligible for this study. The study design of the ABSORB Cohort B is available at the ClinicalTrials.gov website (NCT00856856), whereas the SPIRIT trials have been published elsewhere (12,13). In brief, the common inclusion criteria were patients 18 years of age or older, with a diagnosis of stable or unstable ischemia and with a de novo lesion in a native coronary artery between 50% and 99%. Exclusions included patients with an evolving myocardial infarction, stenosis of an unprotected left main or ostial right coronary artery, presence of intracoronary thrombus, or heavy calcification. Excessive tortuosity proximal to or within the lesion and extreme angulation (>90%) proximal to or within the lesion were also all exclusion criteria.

The ABSORB Cohort B trial included patients treated with BVS. The scaffold is a balloon-expandable device, consisting of a polymer backbone of poly-L-lactide coated with a thin layer of a 1:1 mixture of an amorphous matrix of poly-D,L-lactide polymer containing 100 $\mu g/cm^2$ of the antiproliferative drug everolimus. The implant is radiolucent but has 2 platinum markers at each edge that allow visualization on angiography and other imaging modalities. Physically the scaffold has struts with an approximate thickness of 150 $\mu m$, which are arranged as in-phase zigzag hoops linked together by 3 longitudinal bridges (Fig. 1).

The SPIRIT FIRST and II trials included patients treated with Xience V everolimus-eluting stent (EES) or Multi-Link Vision stent (Abbott Vascular). The metallic platform is constructed by a cobalt chromium alloy; the EES is coated by a permanent polymer and antiproliferative drug. The platform consists of serpentine rings connected by links fabricated from a single piece, with a strut thickness of 81 $\mu m$. In the EES, the polymer and drug coating add a combined thickness of 7 $\mu m$ (Fig. 1).

**Abbreviations and Acronyms**

BVS = bioresorbable vascular scaffold(s)
EES = everolimus-eluting stent(s)
MPS = metallic platform stent(s)
QCA = quantitative coronary angiography
WSS = wall shear stress
2D = 2-dimensional

**Treatment procedure.** Lesions were treated with routine interventional techniques that included mandatory predilation with a balloon shorter and 0.5-mm smaller in diameter than the study device. The BVS was implanted at a pressure not exceeding the rated burst pressure (16 atm). Post-dilation with a balloon shorter than the implanted device was allowed at the discretion of the operator, as was bailout treatment.

**Quantitative coronary angiography (QCA) evaluation.** The operator was requested to select an angiographic view with minimal foreshortening of the lesion and limited overlap with other vessels. This view was used for all phases of the treatment: baseline angiography, pre-dilation, device deployment at maximal pressure, and after devising final result (14). The 2-dimensional (2D) angiograms were analyzed by the core laboratory (Cardialysis, Rotterdam, the Netherlands) with the CASS II analysis system (Pie Medical BV, Maastricht, the Netherlands). In each patient, the treated region and the peri-treated regions (defined by 5 mm proximal and distal to the device edge) were analyzed. The

JACC: CARDIOVASCULAR INTERVENTIONS, VOL. 3, NO. 11, 2010
NOVEMBER 2010:1190–8

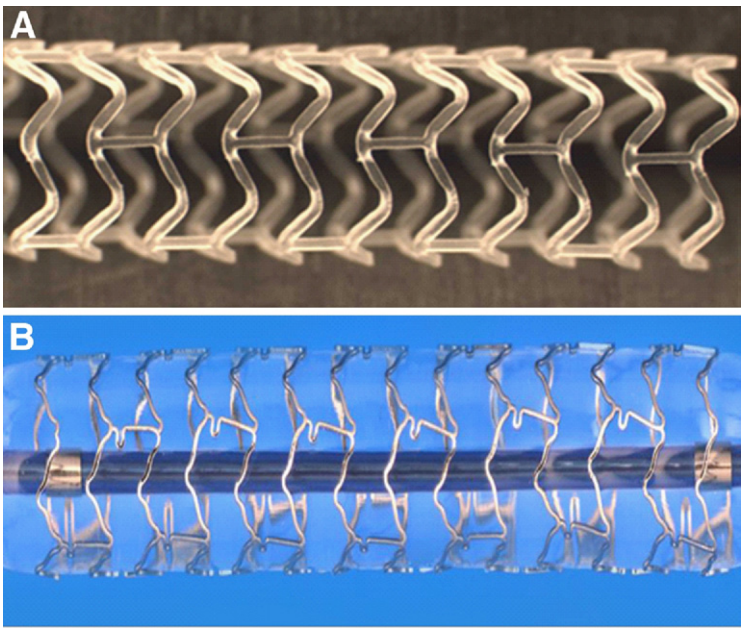


**Figure 1. Structure and Design of Studied Intracoronary Devices**

**(A)** A 1.1 everolimus-eluting bioresorbable vascular scaffold device (BVS) consists of a backbone of poly-L-lactide coated with a thin mixture of poly-D,L-lactide polymer and everolimus. The struts drawn as in-phase zigzag hoops linked together by 3 longitudinal bridges. The strut thickness is 150 $\mu$m. **(B)** Multi-link Vision and Xience V (Abbott Vascular, Santa Clara, California) are the metal platform stents and consist of a metallic platform made of cobalt chromium alloy. The struts drawn as serpentine rings connected by links fabricated from a single piece. The Xience V is covered by a durable fluorinated polymer and everolimus. The strut thickness is 81 $\mu$m.

following QCA parameters were measured: computer-defined minimal luminal diameter, reference diameter obtained by an interpolated method, and percentage diameter stenosis.

With the same views as the core laboratory, the segment of interest was defined as the segment between the 2 nearest side branches that included the treated region. The proximal side branch was used as an index anatomical landmark, and the distance from this branch to the proximal mark of the device in the post-treatment view as well as the device length (post-treatment region) was measured. Then, in the pre-treatment view the pre-treatment region (region to be subsequently treated) was defined at the same distance from the referred side branch and from the post-treatment region (15). The pre-treatment, inflated-balloon, and post-treatment regions were used to measure the curvature and angulation (Fig. 2).

"Curvature" is defined as the infinitesimal rate of change in the tangent vector at each point of the centerline. This measurement has a reciprocal relationship to the radius of the perfect circle defined by the curve at each point. The curvature value is calculated as 1/radius of the circle in $cm^{-1}$ (16), with a research program installed in the QCA Analysis software (CASS II version 1.2 Beta, Pie Medical Imaging). This program has been previously described and tested (17). The software automatically detects the lumen contours of the selected segment and configures the centerline. Three points are then defined according to the centerline: 1 at the proximal, 1 at the distal, and 1 at the center of the defined segment. Next, a perfect circle is drawn through these points, calculating the radius of the circle and the curvature value.

"Angulation" is defined as the angle in degrees that the tip of an intracoronary guidewire would need to reach the distal part of a coronary bend. Angles were measured with the modification of a previously described method (18). In brief, the tangents of the centerlines defined by the 5-mm proximal and distal parts of the analyzed region at the end-diastolic angiographic frame determine the angle (18). This method was shown to have good interobserver agreement ($r = 0.94$, $p < 0.01$) with a methodological error in repeated measures of $<4.2^{\circ}$ (1).

Differences in curvature and angulation were measured in systole and diastole separately as values in the pre-treatment minus values in the post-treatment (Fig. 3). Cyclic changes in vessel curvature and angulation were estimated as differences between systole and diastole at pre-treatment and differences at post-treatment.

**Statistical analysis.** The Kolmogorov-Smirnov test was used to evaluate the normality assumptions of all continuous

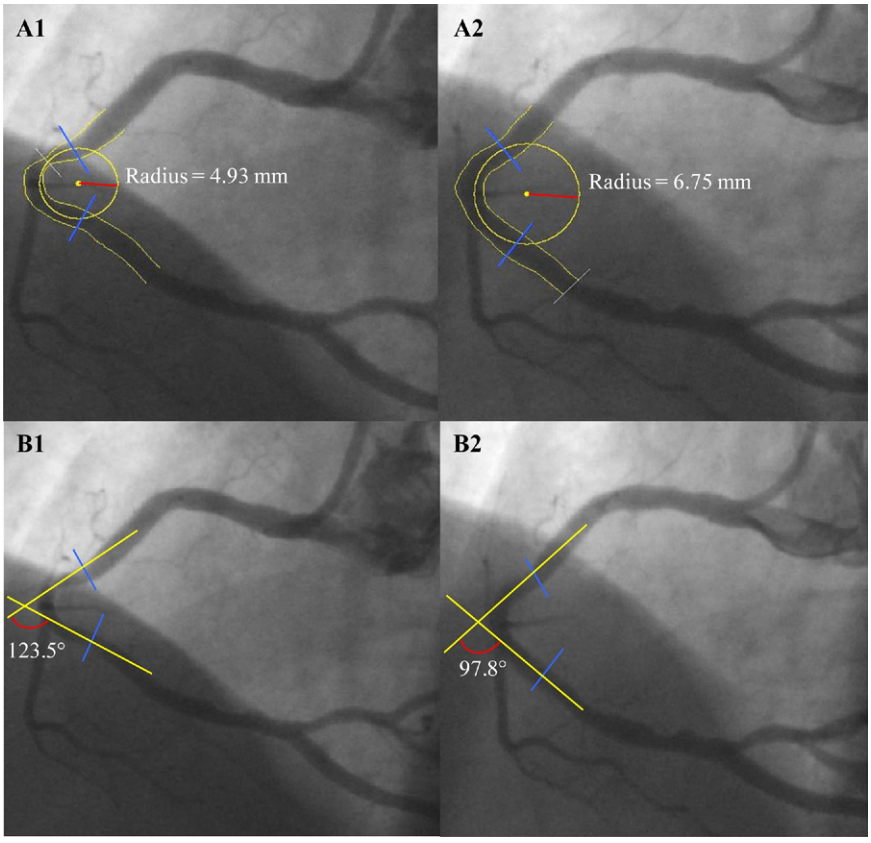


**Figure 2. Curvature and Angulation Analysis**

Curvature **(A)** and angulation **(B)** analysis are shown before deployment **(A1 and B1)** and after deployment **(A2 and B2)**. Curvature is estimated as 1/radius (0.203 $mm^{-1}$ in A1 and 0.148 $mm^{-1}$ in A2). Angulation is defined by the tangents of the centerlines.

variables. Descriptive statistical analysis was performed with continuous variables expressed as median (interquartile range) and with categorical variables presented as counts (percentage). For comparison between groups, 2-tailed *t* tests or Mann-Whitney *U* test were used for the continuous variables according to the Gaussian distribution. The chi-square test has been used to assess differences in categorical variables. Comparisons within groups have been estimated with Wilcoxon or Friedman paired tests.

Because the curvature, angulation, cyclic changes of curvature and angulation, and difference of curvature and angulation between pre- and post-treatment did not have a normal distribution, a square root transformation was performed to achieve a normal distribution. A univariate analysis was performed between curvature and angulation changes with the following variables: age, sex, hypertension, hypercholesterolemia, diabetes, smoking, previous myocardial infarction, previous coronary revascularization, clinical presentation, reference vessel diameter, minimal lumen diameter, diameter stenosis, pre-treatment segment length, pre-treatment curvature and angle, and cyclic changes in curvature and angulation. Variables that were found to be significant at the univariate level were tested with a multivariate linear regression model that included the used device. The thresholds for entry into and removal from the model were 0.1. All statistical tests were carried out at the 5% level of significance. All measures were obtained by SPSS version 15 (SPSS, Inc., Chicago Illinois).

## Results

**Study population.** A flow chart summarizing patient selection is shown in Figure 4. A total of 191 patients were included in this study, of which 89 were treated with the BVS and 102 with the MPS (77 patients received Xience V and 25 received Multilink-Vision stents). Baseline clinical variables are summarized in Table 1. There was no difference in median age or sex. There were significant differences in rates of smoking status (16.9% vs. 32.4%, $p = 0.01$) and a trend of higher hypercholesterolemia in the BVS group (83.1% vs. 72.5%, $p < 0.08$).

JACC: CARDIOVASCULAR INTERVENTIONS, VOL. 3, NO. 11, 2010
NOVEMBER 2010:1190–8

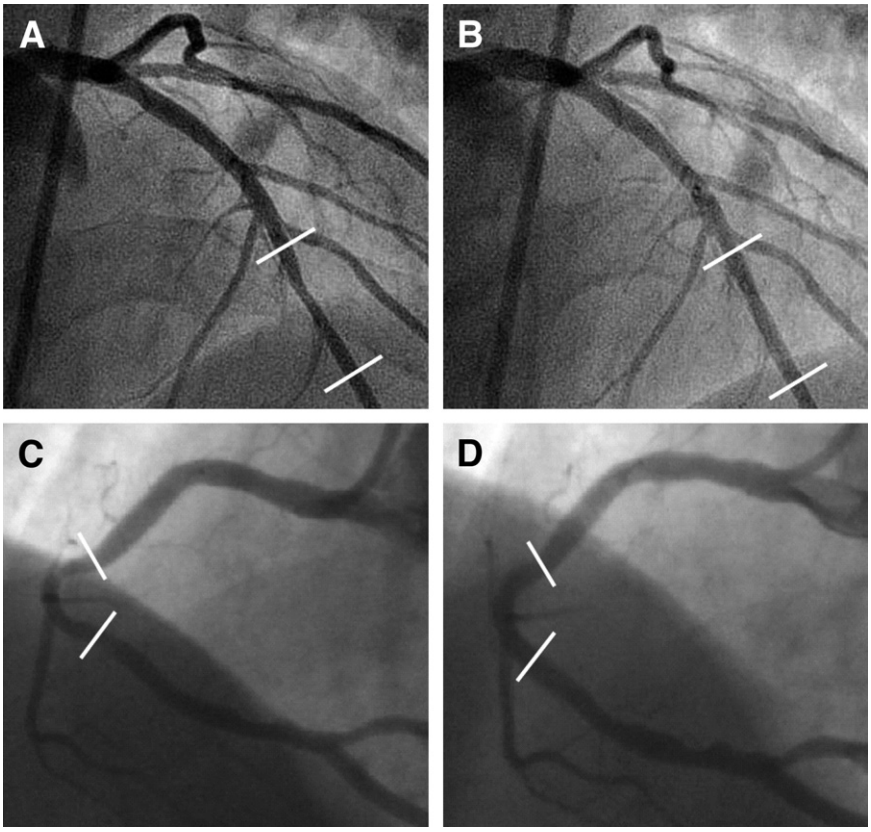


**Figure 3. Changes of Curvature and Angulation**

**(A and B)** Case 1 presents a straight vessel, and Case 2 **(C and D)** presents a curved vessel. Absolute changes in curvature and angulation between pre- **(A and C)** and post-deployment **(B and D)** are small in Case 1 (0.010 $cm^{-1}$ and 5.8°, respectively) and large in Case 2 (0.055 $cm^{-1}$ and 25.7°, respectively).

**Angiographic baseline analysis (pre-treatment).** The left anterior descending artery was the most frequently treated vessel in both groups (44.9% vs. 48.1% in the BVS and MPS, respectively). Quantitative angiographic analysis of the treated lesion showed significant differences between the 2 populations in terms of reference vessel diameter (BVS 2.57 mm vs. MPS 2.80 mm, $p = 0.01$), minimal lumen diameter (BVS 1.03 mm vs. MPS 0.99 mm, $p = 0.03$), and diameter stenosis (BVS 59.0% vs. MPS 63.2%, $p = 0.02$). There was a trend toward shorter lesion length in the BVS group compared with the MPS group (16.3 mm vs. 16.8 mm, $p = 0.06$). There were numerically smaller values of curvature (0.292 $cm^{-1}$ vs. 0.324 $cm^{-1}$, $p = 0.79$) and angulation (29.6° vs. 38.1°, $p = 0.24$) in the BVS group compared with the MPS group (Table 2).

**Geometric changes within and between groups.** Diastolic analysis of the pre-treatment, balloon inflation, and post-treated regions showed significant differences in curvature and angulation between the 3 phases. As expected, the balloon inflated region had the lowest curvature and angulation values (Table 3).

In both groups, there was a significantly lower curvature after treatment than before treatment. The relative median reduction (i.e., from pre-to post-treatment) in curvature was 7.5% in the BVS (from 0.292 to 0.270 $cm^{-1}$, $p < 0.01$), whereas the corresponding reduction with the MPS was 28.7% (from 0.324 to 0.231 $cm^{-1}$, $p < 0.01$). The nonadjusted comparison between the 2 devices in terms of change in curvature showed a nonsignificant trend of less change in the BVS ($p = 0.06$).

As with curvature analysis, angulation changed significantly after deployment. The relative median change of angulation within pre- and post-treatment measures resulted in less modification with the BVS, 13.4% (from 29.6° to 25.6°, $p < 0.01$) versus 25.4% with the MPS (from 38.1° to 28.5°, $p < 0.01$). The nonadjusted comparison between the 2 devices of change in angulation resulted in significantly less modification with the BVS ($p = 0.03$).

Cyclic changes (i.e., between systole and diastole) also showed a significantly lower modification of the hinging movements with the BVS than the MPS after the deployment in curvature ($p = 0.01$) and angulation ($p = 0.04$).

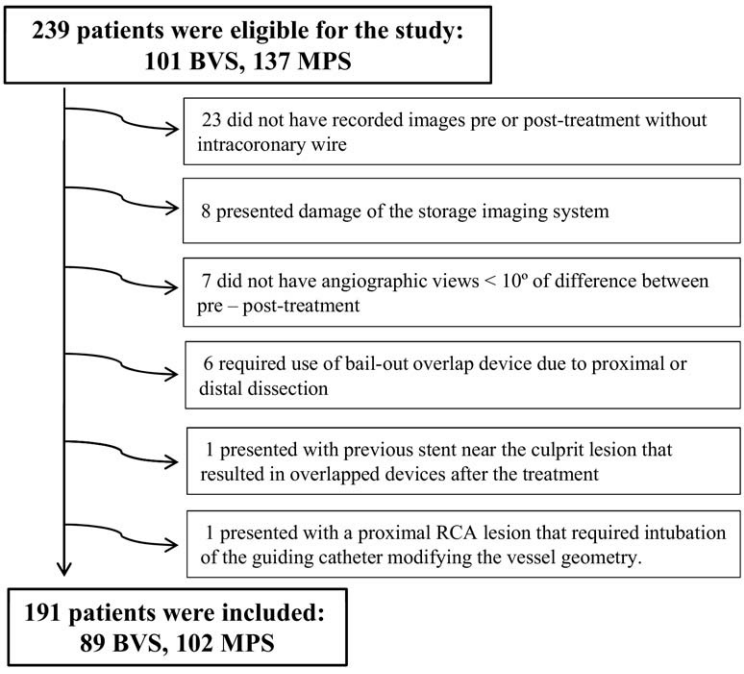


**Figure 4. Flow Chart of Patient Selection**

BVS = everolimus-eluting bioresorbable vascular scaffold(s); MPS = metal platform stent(s); RCA = right coronary artery.

**Geometric changes within and between groups in a subset of patients with more curved and angulated lesions.** To evaluate the changes of curvature and angulation in a subset of patients with more curved and angulated vessels, the population was divided into 2 halves according the median value of the product between curvature and angulation at pre-treatment.

In the group with straight vessels, there were no significant changes between the BVS (absolute median change of 0.005 $cm^{-1}$ of curvature and 3.2° of angulation) and the MPS (absolute median change of 0.003 $cm^{-1}$ and 6.3°, respectively) by p = 0.73 for curvature, and p = 0.18 for angulation. In the group with curved and angulated lesions, there was a significant trend for less modification with the BVS (absolute median change of 0.016 $cm^{-1}$ and 6.3°) than with MPS (absolute median change of 0.026 $cm^{-1}$ and 17.3°) by p = 0.07 of curvature and p = 0.09 of angulation.

**Table 1. Baseline Clinical Variables**

| | BVS (n = 89) | MPS (n = 102) | p Value |
|---|---|---|---|
| Age (yrs) | 63.0 (55.9–69.3) | 62.0 (55.0–71.2) | 0.66 |
| Men | 65 (73.0%) | 70 (68.6%) | 0.51 |
| Hypertension | 56 (62.9%) | 64 (62.7%) | 0.56 |
| Hypercholesterolemia | 74 (83.1%) | 74 (72.5%) | 0.08 |
| Diabetes mellitus | 15 (16.9%) | 16 (15.7%) | 0.83 |
| Smoking history | 15 (16.9%) | 33 (32.4%) | 0.01 |
| Previous AMI | 23 (25.8%) | 28 (27.7%) | 0.55 |
| Previous PCI | 19 (21.3%) | 15 (14.7%) | 0.23 |
| Previous CABG | 2 (2.2%) | 2 (2.0%) | 0.89 |
| Clinical presentation | | | 0.75 |
| Stable or silent angina | 74 (83.1%) | 83 (81.4%) | |
| Unstable angina | 15 (16.9%) | 19 (18.6%) | |

AMI = acute myocardial infarction; BVS = everolimus-eluting bioresorbable vascular scaffold; CABG = coronary artery bypass graft; MPS = metal platform stent; PCI = percutaneous coronary intervention.

**Table 2. Angiographic Baseline Analysis (Pre-Treatment)**

| | BVS (n = 89) | MPS (n = 102) | p Value |
|---|---|---|---|
| Target vessel | | | 0.96 |
| LAD | 40 (44.9%) | 49 (48.1%) | |
| LCX | 20 (22.5%) | 29 (28.4%) | |
| RCA | 29 (32.6%) | 24 (23.5%) | |
| RVD (mm) | 2.57 (2.38–2.82) | 2.80 (2.54–3.00) | 0.01 |
| MLD (mm) | 1.03 (0.85–1.24) | 0.99 (0.73–1.20) | 0.03 |
| Diameter stenosis (%) | 59.0 (53.0–66.0) | 63.2 (54.4–72.0) | 0.02 |
| Pre-treatment region length (mm) | 16.3 (15.0–17.0) | 16.8 (16.1–17.3) | 0.06 |
| Curvature ($cm^{-1}$) | 0.292 (0.179–0.576) | 0.324 (0.159–0.571) | 0.79 |
| Angulation (°) | 29.6 (15.8–55.4) | 38.1 (21.1–60.8) | 0.24 |
| Cyclic changes in curvature ($cm^{-1}$) | 0.097 (0.035–0.190) | 0.091 (0.051–0.173) | 0.95 |
| Cyclic changes in angulation (°) | 4.7 (1.9–11.7) | 6.4 (2.7–11.4) | 0.37 |

LAD = left anterior descending artery; LCX = left circumflex artery; MLD = minimal lumen diameter; RVD = reference vessel diameter; other abbreviations as in Table 1.

JACC: CARDIOVASCULAR INTERVENTIONS, VOL. 3, NO. 11, 2010
NOVEMBER 2010:1190–8

**Table 3. Geometric Changes Within and Between Groups**

| Variable | Device | Pre-Treatment | Balloon | Post-Treatment | Relative Changes Pre vs. Post (%) | p Value* | p Value† | p Value‡ |
|---|---|---|---|---|---|---|---|---|
| Curvature ($cm^{-1}$) | BVS | 0.292 (0.179–0.576) | 0.135 (0.073–0.276) | 0.270 (0.114–0.429) | 7.5 | <0.01 | <0.01 | 0.06 |
| | MPS | 0.324 (0.159–0.571) | 0.117 (0.051–0.272) | 0.231 (0.123–0.400) | 28.7 | <0.01 | <0.01 | |
| Angulation (°) | BVS | 29.6 (15.82–55.4) | 6.8 (1.8–14.8) | 25.6 (12.6–43.1) | 13.4 | <0.01 | <0.01 | 0.03 |
| | MPS | 38.1 (21.1–60.8) | 8.2 (2.8–15.9) | 28.5 (14.5–45.7) | 25.4 | <0.01 | <0.01 | |
| Cyclic changes in curvature ($cm^{-1}$) | BVS | 0.097 (0.035–0.190) | — | 0.072 (0.034–0.155) | 25.8 | 0.82 | — | 0.01 |
| | MPS | 0.091 (0.051–0.173) | — | 0.056 (0.023–0.092) | 38.5 | <0.01 | — | |
| Cyclic changes in angulation(°) | BVS | 4.7 (1.9–11.7) | — | 4.6 (2.2–8.7) | 1.7 | <0.01 | — | 0.04 |
| | MPS | 6.4 (2.7–11.4) | — | 3.8 (1.7–6.3) | 41.0 | <0.01 | — | |

*Comparisons are made within groups comparing pre- and post-treatment values; †comparisons are made within groups comparing pre, balloon, and post-treatment values; ‡comparisons are made between groups comparing the mean changes pre–post of each group.
Abbreviations as in Tables 1 and 2.

**Predictive factors of modifying curvature and angulation.** By univariate analysis, the variables related to changes in curvature were the pre-treatment curvature, cyclic changes of curvature pre-treatment and device. In the multivariate model, the independent predictors of change in curvature were the pre-treatment curvature ($p < 0.01$) and the device used ($p = 0.01$).

By univariate analysis, the variables related to changes in angulation were sex, minimal luminal diameter, diameter stenosis, pre-treatment angulation, cyclic changes of angulation pre-treatment and device. In the multivariate model, the independent predictors of change in angulation were the pre-treatment angulation ($p < 0.01$) and the device used ($p = 0.02$).

## Discussion

The major findings of the study are: 1) the deployment of a 3 × 18 mm BVS and MPS produces significant differences in vessel geometry in terms of curvature and angulation; 2) these changes are significantly less marked for BVS than for MPS, suggesting better conformability of the bioresorbable scaffold; and 3) the pre-treatment curvature and angulation and the type of device are independent predictive factors of vessel changes in curvature and angulation after the deployment.

Our study found that both BVS and MPS modify the baseline vessel curvature. This change was more accentuated in patients with more curved and/or angulated vessels at pre-treatment and in patients who received an MPS. Few studies have investigated the relationship between changes in vessel geometry and clinical outcomes after treatment with metallic stents. One study found that a pre-treatment vessel angulation more than 33.5° (present in 40.3% of the patients) and changes in the vessel angulation of more than 9.1° (present in 42.6% of the patients) were predictors of increased major adverse cardiac events at 10-month follow-up. This was largely driven by the increased risk of angiographic restenosis in these patients treated with a mixture of first-generation bare-metal stents (1). In the present study, the number of patients who had a pre-treatment angulation >33.5° and changes in angulation of >9.1° was 50.3% and 36.6%, respectively.

Nevertheless, some basic science investigations that have focused on the change in flow dynamics and wall shear stress (WSS) have reported that curved vessels have a greater association with turbulent flow and nonuniform distributions of WSS compared with straight vessels. In addition, the outer curvature of a coronary vessel is subjected to a higher WSS, whereas the inner regions have a lower WSS. In native coronary arteries, regions with low WSS have been associated with a higher frequency of atherosclerotic plaques (19,20). This relationship has also been found between low WSS and the development of thick neointimal hyperplasia in bare-metal stents (3) and drug-eluting stents (21). It remains to be investigated whether a fully conformable device will have favorable or unfavorable effects on shear stress.

There is a paucity of data concerning the clinical implications of changes in vessel geometry with metallic stents. Thus, the clinical benefits associated with better conformability of the BVS require further investigation at medium and long-term follow-up and, importantly, should incorporate assessment of shear stress in the clinical setting.

Moreover, other studies have found a paradoxical response to vessel curvature after coronary stenting, with displacement of the vessel curvature present before device implantation, to the edges of the device after deployment. These "inflow" and "outflow" angles might indicate regions of low WSS (2,22).

The fact that the pre-treatment curvature and angulation influence the changes in vessel geometry is intuitive (a straight vessel cannot be straightened further) and has been reported in previous studies (22). The division of our population into 2 halves according to the extent of vessel curvature and angulation showed that the main changes in vessel geometry were observed in the group with the greatest

bending at baseline (Fig. 3). This division has been made arbitrarily with the median value of the product between curvature and angulation at pre-treatment, because there is not a common consensus defining when a vessel is tortuous, curved, or angulated.

The relation between baseline coronary bending and changes in vessel geometry after device deployment and clinical outcomes cannot only be explained by alteration of the flow dynamics and WSS within the vessel. Device implantation in angulated lesions has been related to metal stent fracture, which is a well-recognized cause of restenosis (23). The prevalence of metallic stent fracture ranges from 2.4% to 29.0% in different registries (24,25). In a study that included 3,920 patients, a bend of more than 75° was described as an independent predictor of stent fracture (26). However, in the context of a polymeric device, by design, the struts will eventually fracture as a part of the resorption process.

The most important characteristic that will determine changes in geometry of the vessel wall is the conformability of the device, which might be different between currently commercially available devices. The device conformability will depend on both the design and material of the device (7,8). The comparison of 17 types of bare-metal stents showed that the material and the design were determinants in different stent properties, including conformability (22,27). The Xience V stent has been compared with 7 other different drug-eluting stents in terms of flexibility and was shown to have a flexibility classified in the mid-range of the ranking (7). Similar data regarding the BVS are reported in this study. The materials used by the 2 intravascular devices in this study are different, and it has an important effect on their conformability. In addition, the design pattern is different between the 2 devices (Fig. 1).

**Study limitations.** Despite the use of the least foreshortened view for the 2D angiographic analysis, it is not the most optimal image method to assess the geometry of the coronary vessels. Three-dimensional assessment has been proposed as a better alternative to show better correlation with the true segment length (28). However, the use of 3-dimensional reconstruction from 2D angiograms requires an accurate acquisition, and despite the use of biplane images, sometimes the reconstruction is not possible with the currently available software (29). In our study, the measured median device length after the deployment was 16.2 mm for the BVS and 16.6 mm for the MPS, which represents an estimated foreshortening of 10.0% and 7.8%, respectively, according to the real device length (18 mm). However, the differences between the pre- and post-treatment angiographic views were $<2°$, showing that the analysis has been essentially performed in the same angiographic view.

The software used to assess the curvature computed the centerline according to the luminal contours of the vessel. In case of eccentric lesions, the centerline was still drawn inside the lumen, therefore, the curvature might lead to an under- or overestimation of the real value of the vessel centerline. The inaccuracy occurring because of this is negligible, considering that we are measuring the difference in curvature and angulation in the same angiographic view during diastole. Moreover, the measurement at systole and diastole can be influenced not only by the eccentricity of the culprit lesion, but also by complex coronary shape in the different moments of the cardiac cycle not detected by the 2D analysis.

The presence of calcium might also impact the relationship between vessel geometry and device implantation; however, its contribution is poorly defined. We did not explore this, because it has been demonstrated that there is poor correlation between the inter- and intraobserver detection of calcium on coronary angiography (kappa index of 0.42 and 0.64, respectively) (30). Multislice computed tomography scanning allows better detection of calcium compared with angiography and, moreover, it enables 3-dimensional reconstruction of vessel geometry. Analysis of tissue composition by virtual histology would have been helpful in interpreting the results; however, virtual histology was not performed before scaffold implantation and was not available at all in the SPIRIT patients (31).

## Conclusions

Implantation of a 3 × 18 mm everolimus-eluting BVS results in a significant but modest change in vessel curvature and angulation. This change is more accentuated in vessels with more severe baseline curvature and angulation. Nevertheless, it is clearly much less extensive than that produced by conventional metallic platform stents in the acute phase after deployment, implying better conformability of the BVS. The clinical significance of the observed differences in "conformability" between bioresorbable and metallic platform stents is unclear and will require further investigation.

### Acknowledgments

The authors want to thank Mr. Folkert and the people of Pie Medical for adapting the curvature measure software to the available CASS II program.

**Reprint requests and correspondence:** Dr. Patrick W. Serruys, Ba583a, Thoraxcenter, Erasmus MC,'s-Gravendijkwal 2303015 CE Rotterdam, the Netherlands. E-mail: p.w.j.c.serruys@erasmusmc.nl.

## REFERENCES

1. Gyongyosi M, Yang P, Khorsand A, Glogar D; Austrian Wiktor Stent Study Group and European Paragon Stent Investigators. Longitudinal straightening effect of stents is an additional predictor for major adverse cardiac events. J Am Coll Cardiol 2000;35:1580–89.

2. Wentzel JJ, Whelan DM, van der Giessen WJ, et al. Coronary stent implantation changes 3-D vessel geometry and 3-D shear stress distribution. J Biomech 2000;33:1287–95.
3. Wentzel JJ, Krams R, Schuurbiers JC, et al. Relationship between neointimal thickness and shear stress after Wallstent implantation in human coronary arteries. Circulation 2001;103:1740–5.
4. Ino Y, Toyoda Y, Tanaka A, et al. Predictors and prognosis of stent fracture after sirolimus-eluting stent implantation. Circ J 2009;73: 2036–41.
5. Colombo A, Stankovic G, Moses JW. Selection of coronary stents. J Am Coll Cardiol 2002;40:1021–33.
6. Ormiston JA, Dixon SR, Webster MW, et al. Stent longitudinal flexibility: a comparison of 13 stent designs before and after balloon expansion. Catheter Cardiovasc Interv 2000;50:120–4.
7. Schmidt W, Lanzer P, Behrens P, Topoleski LD, Schmitz KP. A comparison of the mechanical performance characteristics of seven drug-eluting stent systems. Catheter Cardiovasc Interv 2009;73: 350–60.
8. Sangiorgi G, Melzi G, Agostoni P, et al. Engineering aspects of stents design and their translation into clinical practice. Ann Ist Super Sanita 2007;43:89–100.
9. Serruys PW, Ormiston JA, Onuma Y, et al. A bioabsorbable everolimus-eluting coronary stent system (ABSORB): 2-year outcomes and results from multiple imaging methods. Lancet 2009;373:897–910.
10. Ormiston JA, Serruys PW, Regar E, et al. A bioabsorbable everolimus-eluting coronary stent system for patients with single de-novo coronary artery lesions (ABSORB): a prospective open-label trial. Lancet 2008; 371:899–907.
11. Onuma Y, Serruys PW, Ormiston JA, et al. Three-year results of clinical follow-up after a bioresorbable everolimus-eluting scaffold in patients with de novo coronary artery disease: the ABSORB trial. EuroIntervention 2010;6:447–53.
12. Serruys PW, Ong AT, Piek JJ, et al. A randomized comparison of a durable polymer everolimus-eluting stent with a bare metal coronary stent: the SPIRIT first trial. EuroIntervention 2005;1:58–65.
13. Serruys PW, Ruygrok P, Neuzner J, et al. A randomised comparison of an everolimus-eluting coronary stent with a paclitaxel-eluting coronary stent: the SPIRIT II trial. EuroIntervention 2006;2:286–94.
14. Tanimoto S, Serruys PW, Thuesen L, et al. Comparison of in vivo acute stent recoil between the bioabsorbable everolimus-eluting coronary stent and the everolimus-eluting cobalt chromium coronary stent: insights from the ABSORB and SPIRIT trials. Catheter Cardiovasc Interv 2007;70:515–23.
15. Sabate M, Costa MA, Kozuma K, et al., Dose Finding Study Group. Methodological and clinical implications of the relocation of the minimal luminal diameter after intracoronary radiation therapy. J Am Coll Cardiol 2000;36:1536–41.
16. Choi G, Cheng CP, Wilson NM, Taylor CA. Methods for quantifying three-dimensional deformation of arteries due to pulsatile and nonpulsatile forces: implications for the design of stents and stent grafts. Ann Biomed Eng 2009;37:14–33.
17. Reiber JH, Serruys PW. Advances in Quantitative Coronary Arteriography (Developments in Cardiovascular Medicine). Dordrecht, the Netherlands: Kluwer Academic Publishers, 1992.
18. Ellis SG, Topol EJ. Results of percutaneous transluminal coronary angioplasty of high-risk angulated stenoses. Am J Cardiol 1990;66: 932–7.
19. Asakura T, Karino T. Flow patterns and spatial distribution of atherosclerotic lesions in human coronary arteries. Circ Res 1990;66: 1045–66.
20. Wentzel JJ, Janssen E, Vos J, et al. Extension of increased atherosclerotic wall thickness into high shear stress regions is associated with loss of compensatory remodeling. Circulation 2003;108:17–23.
21. Gijsen FJ, Oortman RM, Wentzel JJ, et al. Usefulness of shear stress pattern in predicting neointima distribution in sirolimus-eluting stents in coronary arteries. Am J Cardiol 2003;92:1325–8.
22. Liao R, Green NE, Chen SY, et al. Three-dimensional analysis of in vivo coronary stent—coronary artery interactions. Int J Cardiovasc Imaging 2004;20:305–13.
23. Lee SH, Park JS, Shin DG, et al. Frequency of stent fracture as a cause of coronary restenosis after sirolimus-eluting stent implantation. Am J Cardiol 2007;100:627–30.
24. Okumura M, Ozaki Y, Ishii J, et al. Restenosis and stent fracture following sirolimus-eluting stent (SES) implantation. Circ J 2007;71: 1669–77.
25. Nakazawa G, Finn AV, Vorpahl M, et al. Incidence and predictors of drug-eluting stent fracture in human coronary artery a pathologic analysis. J Am Coll Cardiol 2009;54:1924–31.
26. Shaikh F, Maddikunta R, Djelmami-Hani M, Solis J, Allaqaband S, Bajwa T. Stent fracture, an incidental finding or a significant marker of clinical in-stent restenosis? Catheter Cardiovasc Interv 2008;71:614–8.
27. Rieu R, Barragan P, Garitey V, et al. Assessment of the trackability, flexibility, and conformability of coronary stents: a comparative analysis. Catheter Cardiovasc Interv 2003;59:496–503.
28. Messenger JC, Chen SY, Carroll JD, Burchenal JE, Kioussopoulos K, Groves BM. 3D coronary reconstruction from routine single-plane coronary angiograms: clinical validation and quantitative analysis of the right coronary artery in 100 patients. Int J Cardiovasc Imaging 2000;16:413–27.
29. Bruining N, Tanimoto S, Otsuka M, et al. Quantitative multi-modality imaging analysis of a bioabsorbable poly-L-lactic acid stent design in the acute phase: a comparison between 2- and QCA, QCU and QMSCT-CA. EuroIntervention 2008;4:285–91.
30. Popma JJ, Lansky AJ, Yeh W, et al. Reliability of the quantitative angiographic measurements in the New Approaches to Coronary Intervention (NACI) registry: a comparison of clinical site and repeated angiographic core laboratory readings. Am J Cardiol 1997;80:19K–25K.
31. Rumberger JA, Simons DB, Fitzpatrick LA, Sheedy PF, Schwartz RS. Coronary artery calcium area by electron-beam computed tomography and coronary atherosclerotic plaque area. A histopathologic correlative study. Circulation 1995;92:2157–62.

**Key Words:** angulation ■ bioresorbable ■ curvature ■ conformability ■ stent.